CFD Simulation of Pore Pressure Oscillation Method for the Measurement of Permeability in Tight Porous-Media

Seyed Armin Madani[1], Mehdi Mokhtari[*2], Abdennour Seibi[3]
[1]Oil Center Research, Lafayette, LA, USA.
[2,3]Petroleum Engineering Department, University of Louisiana at Lafayette, Lafayette, LA, USA.
*Petroleum Engineering Department, University of Louisiana at Lafayette, P.O. Box: 44690, Lafayette, LA 70504
Email: mokhtari.mehdi@louisiana.edu

Abstract: Accurate estimation of rock permeability and porosity play a crucial role in the evaluation of oil and gas reservoirs. This evaluation is however, challenging in tight formations such as shale due to the slow transition of fluid in such formations with extremely-low permeability. To overcome the long experimental time of conventional techniques for permeability measurement (steady-state methods), transient methods such as pore pressure oscillation method has been proposed for laboratory measurement of permeability in tight formations. In this method, sinusoidal pore pressure oscillation is applied at upstream side of reservoir core sample and the response of the sample at the downstream side is evaluated. In this paper, the experimental technique for permeability and porosity measurement is simulated using CFD module of COMSOL Multiphysics and the results are compared with analytical solutions. An excellent agreement between CFD and analytical data is observed and the results are analyzed and discussed in details. Finally, two different scenarios are defined for 6 heterogeneous samples and the response of this technique to such cases are analyzed and studied.

Keywords: Permeability, Porosity, Pressure Oscillation Method, CFD, Tight Formation.

1. Introduction

By advances in technology and knowledge of petroleum engineering, geology, and geophysics, unconventional reservoirs have become relatively a considerable portion of oil and gas resources around the world. Tight gas sands, oil and gas shales, and coalbed methane are examples of unconventional reservoirs. The word unconventional comes from the fact that these reservoirs have extremely low permeability and they need special recovery operations outside of the conventional recovery practices to extract the existing hydrocarbons. Accurate evaluation of porosity and permeability plays a crucial role in reservoir characterization since these two parameters are used to estimate the reservoir drainage area and optimize the well spacing, drilling, completion, and production procedures [1]. For tight reservoir samples, conventional core analysis techniques are not practical due to very low permeability and very long flow transition time in the core samples.

Core analysis techniques can be categorized into two groups of steady state (SS) and unsteady state (USS) techniques. In SS methods, permeability can be calculated from Darcy's equation by applying a constant pressure head or a constant fluid flow rate at one side of the core and monitoring the established flow rate or pressure head at both sides. In case of using SS methods for tight samples, apart from requiring a long time (days or even weeks) to get an established flow along the sample, the imposed high pressure gradient creates considerable stress fields inside the core samples. Depending on the core mechanical properties, stress fields can change the structure of the core, which can result in inaccurate measurement of permeability and porosity. To show the importance of considering the effects of high pore pressure on formation characterization, Mokhtari et. al. investigated the stress dependent permeability, anisotropy, and wettability of shale samples and presented the effect of stress on the permeability of such fractured reservoirs [2].

Pulse-Decay method as the first USS or transient method was developed and used by Brace et al at 1968 [3]. Later, Boinott used the complex pore pressure transient method to measure the permeability of rocks and examined the ability of this method to use them for samples with higher permeability [4]. Generally, USS methods are developed mathematically based on analyzing the transient response of pressure at the downstream side of core to the pressure perturbation (e.g. step or sinusoidal pressure variation) at the upstream side of it [5][6]

therefore, they can be conducted in a considerably shorter period of time compared to SS methods [7][8]. In pressure oscillation technique, a sinusoidal variation in pressure with a specific frequency and amplitude (which is usually less than 10% of pore pressure) gets applied at the upstream side of the core. The pressure response at the downstream side will be a sinusoidal wave with the frequency but with a phase shift and attenuated amplitude.

The pressure response at the downstream is initially a combination of transient response (exponential decay) and steady state response (sinusoidal). The transient part eventually fades away and only the steady state sinusoidal wave gets observed. Therefore, the pore pressure oscillation technique can be considered as a combination of both SS and USS techniques. Pressure oscillation method was originally developed as an extension of a method for measuring hydraulic diffusivity by Kranz et. al. [9]. Later, the theoretical background, data analysis, and design considerations in experiments, were discussed in details by Fischer [10]. Bernabé et. al. rearranged the analytical formulation and redefined the amplitude attenuation and phase shift of downstream pressure wave as functions of dimensionless permeability and dimensionless porosity [11]. Song and Renner applied pressure analysis and flow analysis methods to evaluate the application of pore pressure oscillation method on two Fontainebleau sandstone samples [12]. Bennion and Goss examined the theory and presented correlations to design sinusoidal pressure experiments to get the frequency response data and characterize the porous medium and its fluid properties [13].

However, in case of very low permeability samples, the pressure response at the downstream side can be greatly affected by the variations in temperature during the course of experiment and also by the existing noises from the lab instruments or the surrounding environment. In the other words, even small magnitudes of error in reading the pressure response at the downstream side can lead to inaccuracies in estimation of porosity and permeability. In addition, the theories behind these techniques are derived based on the assumptions of homogeneity and isotropy of samples which are not valid in many cases. Mokhtrai and Tutuncu showed the importance of accurate determination of permeability in shale samples due to anisotropy [14], heterogeneous nature of shale formations, presence of lamination, and existence of induced or natural fractures in their structure [15] it is still challenging to accurately measure their properties. Due to complexity of including the different effects such as temperature, heterogeneity, and anisotropy in analytical formulation of oscillation pressure methods, it is not possible to study their effect by analytical techniques.

Computational Fluid Dynamics (CFD) as a cheap and robust tool can be always utilized to mimic physical conditions that are impossible, difficult or very time consuming to be modeled in laboratory experiment. Petroleum engineering as well as other engineering fields is benefiting from the advantages of CFD and numerical simulations. Salehi et. al. utilized CFD to model the formation of filter cake on wellbore core surface [16] and Mokhtari used CFD to characterize the anisotropy in organic-rich shale [15].

In this paper, we simulated the experimental pressure oscillation technique for permeability and porosity characterization using CFD module of COMSOL Multiphysics. We compared the results with analytical solutions to validate and initiate the applications of CFD for further researches on measurement of permeability and porosity in samples not fit to the assumptions of analytical formulations of this technique. In next sections, the theoretical background and derivation of analytical solutions for the flow governing equations, the methodology, the simulation results, and the effect of different core and operational parameters in experiments are presented and discussed in details.

2. Methodology

2.1 Analytical Formulation

In pressure oscillation method, a sinusoidal pressure wave is applied at the upstream side of the core and once it travels through the porous media of core sample, its amplitude attenuates and its phase shifts. These two parameters are unique for samples with different porosity and permeability therefore, by having the analytical formula for the amplitude attenuation and phase shift as a function of permeability and porosity, these two variables can be calculated based on the

experimental results. The continuity and Darcy flow equation in porous media can be defined as:

$$\frac{\partial(\varphi\rho)}{\partial t}+\frac{\partial(\rho u)}{\partial x}=0 \quad (1)$$

$$u=-\frac{k}{\mu}\frac{dp}{dx} \quad (2)$$

where φ, p, ρ, u, k, and μ are porosity, pressure, density, flow velocity, permeability, and viscosity respectively. Assuming ideal gas and combining (1) and (2) we get:

$$\varphi\frac{\partial\rho}{\partial t}-\frac{k}{\mu}\frac{\partial}{\partial x}(\rho\frac{\partial p}{\partial x})=0 \quad (3)$$

Based on the assumption of ideal gas we have $\frac{\partial\rho}{\partial t}=\frac{\rho}{p}\frac{\partial p}{\partial t}$ therefore, by rearranging (3) and defining $\beta_s=\varphi/p$ as the storage capacity, equation (3) can be rewritten as:

$$\frac{\partial p}{\partial t}-\frac{k}{\mu\beta_s}\frac{\partial^2 p}{\partial x^2}=0 \quad (4)$$

In fact, equation (4) is the diffusion equation which defines the change in pressure with respect to time and distance along the core sample. In a sample with length L, the upstream boundary condition for pressure with frequency ω, is defined by a sinusoidal pressure function of time:

$$p(L,t)=P_A\sin(\omega t+\delta),\quad x=L \quad (5)$$

where, P_A and δ are pressure wave amplitude at upstream reservoir and the pressure wave initial phase. At downstream, boundary condition can be defined by combining ideal gas equation with Darcy's equation. From the Darcy equation and the assumption of ideal gas at a downstream reservoir with the volume of V_D we have:

$$\frac{dV}{dt}=-\frac{kA}{\mu}\frac{\partial p}{\partial x} \quad (6)$$

$$\frac{dV}{dt}=\frac{V_D}{p}\frac{dp}{dt} \quad (7)$$

Defining $\beta_d=V_D/p$ as the storage of downstream reservoir (the required volume of fluid at pressure p to cause one unit change in pressure), equations (6) and (7) can be combined and the governing condition at the downstream boundary can be derived as:

$$\frac{dp}{dt}-\frac{kA}{\mu\beta_d}\frac{\partial p}{\partial x}=0,\quad x=0 \quad (8)$$

Using Laplace transformation and Brownian integral for the inverse Laplace transformation [10], the permanent and transient solutions of equation (4) can be defined as [10]:

$$p=\alpha P_A\sin(\omega t+\delta+\vartheta) \quad (9)$$
$$+2P_A\frac{k}{\mu}\beta_S AL$$
$$\sum_{n=1}^{\infty}\left\{\frac{(\beta_S L^2\omega\cos\delta-\frac{k}{\mu}\psi_n^2\sin\delta)[\cos(\xi\psi_n)-\frac{\beta_d\psi_n}{\beta_S AL}\sin(\xi\psi_n)]}{((\frac{k}{\mu})^2\psi_n^4+\beta_S^2L^4\omega^2)[(\beta_d\psi_n^2+\beta_S AL)\cos\psi_n+(\beta_S AL+2\beta_d)\sin\psi_n]}\right.$$
$$\left.\psi_n^2 e^{-\frac{k\psi_n^2}{\mu\beta_S L^2}t}\right\}$$

In permanent part of solution, α and ϑ are the pressure wave amplitude attenuation and pressure wave phase shift at downstream which are defined by [10]:

$$\alpha=\left|\frac{\sqrt{\frac{\beta_s\omega\mu}{2k}}(1+i)\cosh[\sqrt{\frac{\beta_s\omega\mu}{2k}}(1+i)x]+\frac{\beta_d i\omega\mu}{kA}\sinh[\sqrt{\frac{\beta_s\omega\mu}{2k}}(1+i)x]}{\sqrt{\frac{\beta_s\omega\mu}{2k}}(1+i)\cosh[\sqrt{\frac{\beta_s\omega\mu}{2k}}(1+i)L]+\frac{\beta_d i\omega\mu}{kA}\sinh[\sqrt{\frac{\beta_s\omega\mu}{2k}}(1+i)L]}\right| \quad (10)$$

$$\vartheta=\arg\left\{\frac{\sqrt{\frac{\beta_s\omega\mu}{2k}}(1+i)\cosh[\sqrt{\frac{\beta_s\omega\mu}{2k}}(1+i)x]+\frac{\beta_d i\omega\mu}{kA}\sinh[\sqrt{\frac{\beta_s\omega\mu}{2k}}(1+i)x]}{\sqrt{\frac{\beta_s\omega\mu}{2k}}(1+i)\cosh[\sqrt{\frac{\beta_s\omega\mu}{2k}}(1+i)L]+\frac{\beta_d i\omega\mu}{kA}\sinh[\sqrt{\frac{\beta_s\omega\mu}{2k}}(1+i)L]}\right\} \quad (11)$$

where,

k = the permeability of core sample
ω = the frequency of pressure wave
x = the distance from downstream reservoir
t = the time at experiment
P_A = the amplitude of oscillated pressure wave
A = the cross-sectional area of core sample
μ = the viscosity of pore fluid
β_d = the storage of downstream reservoir

and ψ_n is the roots of

$$\tan\psi=\frac{\beta_s AL}{\beta_d\psi} \quad (12)$$

β_s or the sample storage capacity is defined as the combination of C_b (the bulk compressibility of the core sample), C_f (the compressibility of core fluid), C_r (the compressibility of core sample rock), and ϕ (the porosity of core sample) [3]:

$$\beta_s=C_b+\phi C_f-(1+\phi)C_r \quad (13)$$

In order to simplify equations (10) and (11), the dimensionless porosity ξ and the dimensionless permeability η can be defined as:

$$\xi=\frac{AL\beta_s}{\beta_d},\quad \eta=\frac{ATk}{\pi L\mu\beta_d} \quad (14)$$

$$A_r e^{-i\theta}=(\frac{1+i}{\sqrt{\xi\eta}}\sinh[(1+i)\sqrt{\frac{\xi}{\eta}}+\cosh[(1+i)\sqrt{\frac{\xi}{\eta}})^{-1} \quad (15)$$

where A_r is the upstream to downstream pressure wave amplitude ratio $(0 < A_r < 1)$ and θ is the phase shift of downstream pressure wave with respect to upstream pressure wave phase.

2.2 Experimental Procedure

Figure 1 shows the schematic diagram of experimental setup. Before starting the test, the sample gets stabilized at pore pressure P_0 and then a sinusoidal pressure wave with known amplitude (5% to 10% of pore pressure P_0) and initial phase is applied to the upstream side of a core plug, placed inside a core holder and confined by pressure P_c. In downstream side, the pressure value is recorded and by comparing it to its values at upstream side, the pressure wave amplitude attenuation and pressure wave phase shift gets calculated. Then, based on known values of core sample cross section area A, length of sample L, pressure wave period T, viscosity of pore fluid μ, and storage of downstream reservoir β_d, the values of porosity ϕ and permeability k get calculated from equation (15).

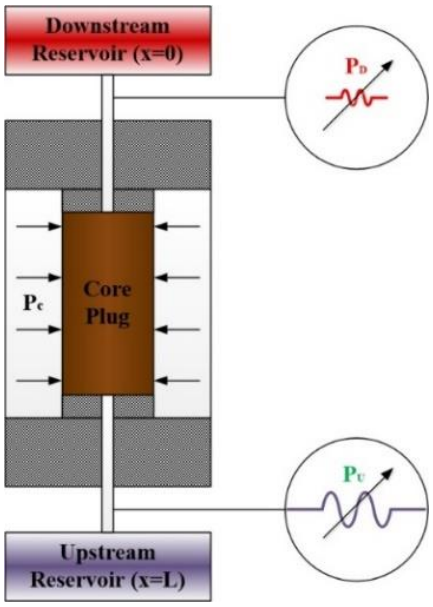

(a)

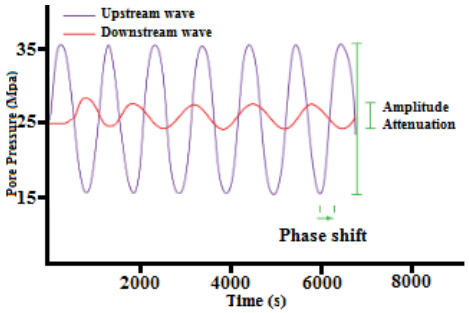

(b)

Figure 1: Schematic diagram of experimental setup (a), an example of pressure data recorded at upstream and downstream reservoirs (b) [17].

At the beginning of pressure data recording in downstream, the pressure response is always a combination of permanent and transient responses. Therefore, in order to obtain the amplitude attenuation and phase shift only from the permanent pressure response and to have the effects of transient part faded away, it is required to do the experiment and record the data for at least several periods of pressure wave.

2.3 CFD Modeling

We used time dependent solvers of COMSOL to simulate flow through porous media. The governing transport equations are conservation of mass and Darcy equations:

$$\frac{\partial}{\partial t}(\varphi\rho) + \nabla.(\rho u) = 0 \qquad (16)$$

$$u = -\frac{k}{\mu}\nabla p \qquad (17)$$

where φ, ρ, u are porosity of porous domain, density of pore fluid, and the velocity of fluid. To mimic the experimental setup conditions and by considering that the volume of upstream reservoir has no effect on pressure response at downstream side, we created the geometry of CFD model from two parts of core plug and downstream reservoir. Core plugs are cylindrical so, the flow inside the core is symmetric and uniform over the cross section of core. As a result, a 2D model can be used to accurately capture the physics of problem and save the computational time. Figure 2 shows the COMSOL CFD model with a medium mesh resolution (created by mapped mesh feature of COMSOL and based on the defined distributions on each face) as well as the defined boundary

conditions. In CFD models, we did not consider the effects of existing stresses generated by the pore pressure on permeability and porosity of model. Therefore, there was no need to define the confining pressure for the model and "no-flow" boundary condition could mimic the conditions at all surrounding boundaries except the upstream boundary. At upstream, the pressure wave was defined by the user as $p = cP_o \sin(\omega t + \delta_0)$ where c, P_o, ω, t, and δ_0 are pore pressure wave amplitude ratio, pore pressure, pressure wave frequency, time, and initial phase of pressure wave.

(a)

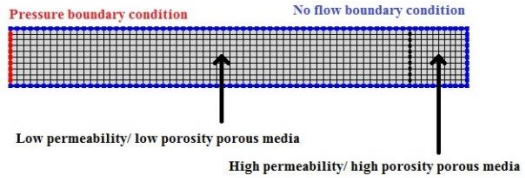

(b)

Figure 2: COMSOL model geometry (a), created computational mesh over the model domain (b).

At the interface of core plug and downstream reservoir, an abrupt change in media's characteristics might result in divergence of solution especially when the core porosity and permeability are very low and the pressure is high. In these cases, the discontinuity in physics of porous media causes high gradients in velocity profiles at this interface and results in limitations for transient simulation time stepping. As the result, in order to avoid stability issues, smaller time steps are required and overall time of simulation will be much longer. In this case, we defined the downstream reservoir as a second porous media as a high porosity ($\varphi > 0.9$) and high permeability ($k > 10^{-6} m^2$) porous media. Defining the downstream reservoir high porosity and permeability, not only can mimic the reservoir as an almost non-porous media but also, improves the stability of solution and results in several times faster convergence of solution. It is just important to consider the real volume of downstream reservoir in calculations using analytical formulations. The Multifrontal Massively Parallel sparse direct Solver (MUMPS) was used as the time dependent direct solver to solve the governing equations for a single phase gas flow. In fluid properties section, the density of fluid can be either defined as ideal gas or the density can be directly defined by the user as $\rho = \rho_0 p / p_0$. In matrix properties section, based on the assumptions of homogenous and isotropic porous media in analytical formulation, the value of permeability should be defined as isotropic permeability.

3. Results and Discussion

3.1 CFD Model verification

In this section, we investigate the application of CFD in modelling pressure oscillation method for homogenous and isotropic cases. A good agreement of simulation results with analytical data can guarantee the application of CFD for modelling and studying the details of pressure oscillation method for more complex cases like heterogeneous and anisotropic core plugs where the existing analytical formulations are not valid. In fact, equations (10) and (11) are derived based on simplification assumptions of homogeneity and isotropy of core plug. A good number of cases with different permeability and porosity were defined and modeled under different downstream reservoir sizes and pressure wave frequency to verify the accuracy of CFD in capturing the physics of problem. Table 1 shows the details of each simulated case.

Table 1: Defined COMSOL CFD models.

Model	$k\,(m^2)$	φ	$L_D\,(mm)$	$T\,(s)$
1	10^{-18}	0.06	50	1200
2	10^{-18}	0.06	50	2400
3	10^{-18}	0.06	25	1200
4	10^{-18}	0.06	25	2400
5	10^{-18}	0.06	5	1200
6	10^{-18}	0.06	5	2400
7	10^{-17}	0.09	50	600
8	10^{-17}	0.09	50	1200
9	10^{-17}	0.09	25	600
10	10^{-17}	0.09	25	1200
11	10^{-17}	0.09	5	600
12	10^{-17}	0.09	5	1200

Other parameters such as length of core plug L, magnitude of pore pressure P_0, amplitude of pressure wave at upstream $A_{upstream}$, and the viscosity of pore fluid μ are kept constant for all models and are summarized in Table 2.

Table 2: Parameters of COMSOL CFD models.

$L(mm)$	$P_0(pa)$	$A_{upstream}(pa)$	$\mu(pa.s)$
50	5×10^6	5×10^5	1.76×10^{-5}

In order to be consistent in modeling, each model was simulated by the time dependent solver for 36 cycles of its wave period using time steps of 1 second and at post-processing the values of amplitude attenuation ratio (ratio of pressure wave amplitude at upstream to its value at downstream) and phase shift were calculated. The number of cells in sample part was 50 for all models and depending on size of downstream reservoir, the number of cells at downstream are 5, 25, and 50. Figure 3 shows the comparison of pressure data at downstream for CFD model and analytical solution during the entire time of modeled test.

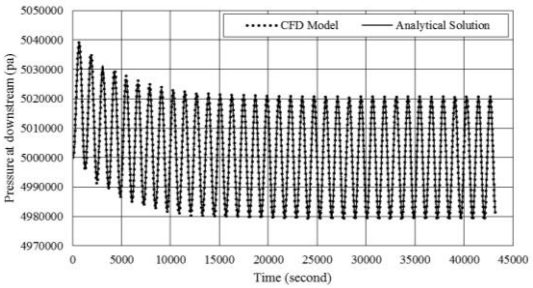

Figure 3: Comparison of CFD and analytical solution for the model with permeability of 10^{-18} m^2 porosity of 0.06, pressure wave period of 1200 seconds, and downstream reservoir length of 25 mm.

As it can be seen in Figure 3, not only the details of permanent part of solution such as amplitude attenuation and phase shift are perfectly captured with CFD model but also, the attenuation of transient pressure magnitude (in first 12 period of wave) is in very good agreement with analytical solution. Based on this excellent agreement, we only compared the values of amplitude attenuation and phase shift of CFD models and analytical solutions for other models.

Figures 4 and 5 summarize the results of all 12 models (listed in Table 1) for various values of A_r (the upstream to downstream pressure wave amplitude). As it was expected, for the same wave period size of downstream reservoir, the higher the permeability and porosity, the higher pressure wave ratio and phase shift will be. As it can be seen from Figures 4 and 5, the negligible difference of results justifies the application of CFD in modeling pressure wave oscillation technique for calculation of permeability and porosity.

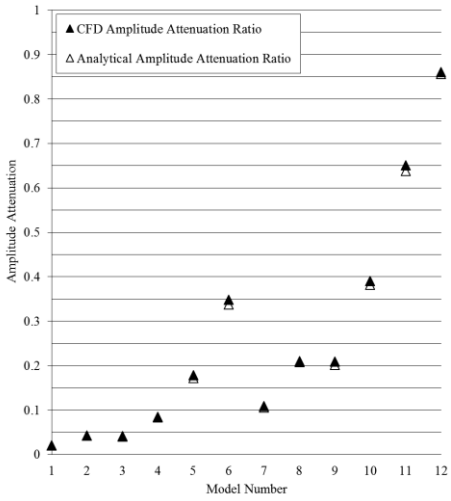

Figure 4: Comparison of amplitude attenuation in CFD models and analytical solution results.

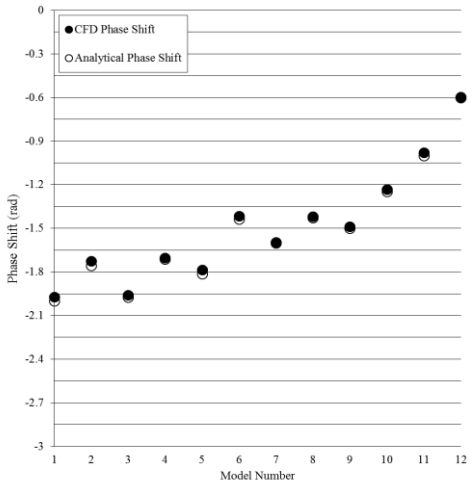

Figure 5: Comparison of phase shift in CFD models and analytical solution results.

Table 3 summarizes the values of relative error (calculated based on equation (18)) for CFD model in both amplitude and phase shift of downstream pressure wave.

$$E(\%)=\left|\frac{CFD\,value-analytical\,solution\,value}{analytical\,solution\,value}\right|\times100 \qquad (18)$$

The maximum error value of 3.79% for pressure wave amplitude and 2.23% for phase shift show the accuracy of CFD and our COMSOL model in capturing the physics of the problem.

Table 3: Relative error of CFD models.

Model number	Wave amplitude error (%)	Phase shift error (%)
1	1.94	1.40
2	1.09	1.72
3	3.28	0.87
4	1.33	0.63
5	3.54	1.61
6	2.95	1.40
7	2.99	0.26
8	1.08	0.73
9	3.79	0.99
10	2.42	1.28
11	1.97	2.23
12	0.51	1.10

Information in Tables 3 shows that in most of the CFD models with same permeability and porosity, the magnitude of both amplitude attenuation error and phase shift error, decrease once the period becomes longer. This may due to having smaller gradients of pressure and velocity along the model domain and it shows the importance of using smaller time steps for models with smaller wave periods or higher frequencies.

Figure 6 shows the amplitude attenuation and phase shift for the pressure wave in different locations along the core in model 8 of Table 1.

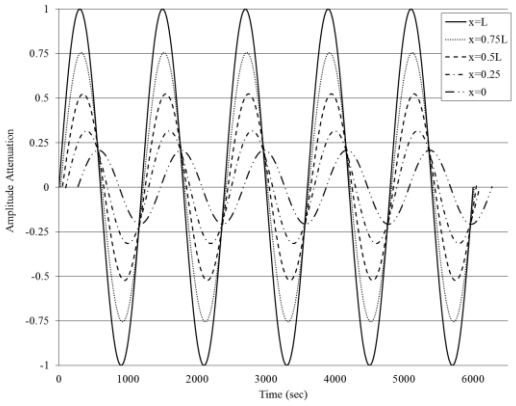

Figure 6: Pressure wave along length of core sample (model No. 8).

The pressure profiles in Figure 6 are for steady state part of solution (no transient effect exists) and they show the nonlinear attenuation of wave amplitude and phase shift along core sample.

3.2 Heterogeneous CFD Models

In order to study the physics and behavior of pressure oscillation method in heterogeneous core samples, three different heterogeneity scenarios (different arrangement of layers) were defined and simulated for two different sets of permeability and porosity. In all models, the total length of core sample is $L = 50\,mm$, the pressure wave period is $\omega = 2400\,s$, and the length of downstream reservoir is $L_D = 5\,mm$, the initial pore pressure is $p = 5 \times 10^6\ Pa$. Figure 7 shows the geometry and details of permeability and porosity for each model. Layers number 1 have the permeability of $k = 10^{-18}\,m^2$ and porosity of $\varphi = 0.06$ while layers number 2 and number 3 have permeability and porosity values of $k = 10^{-17}\,m^2$, $\varphi = 0.09$ and $k = 10^{-16}\,m^2$, $\varphi = 0.1$ respectively. The length of layers 2 and layers 3 is $10\,mm$ and the length of layers 1 in models 1, 3, 5, and 6 is $40\,mm$ and it is $20\,mm$ in models 2 and 4.

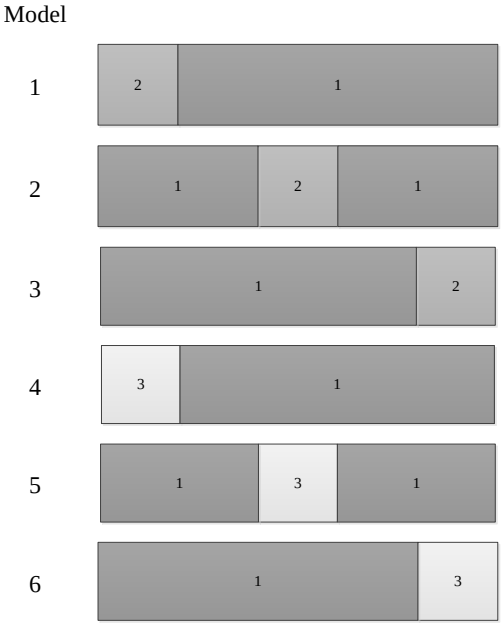

Figure 7: Heterogonous models geometry.

All 6 models were simulated using the same modeling techniques for homogeneous cases and the results of amplitude attenuation and phase shift in downstream reservoir location are summarized in Table 4.

Table 4: results of heterogeneous CFD models.

Model number	Amplitude attenuation	Phase shift
1	0.358	-1.376
2	0.345	-1.470
3	0.310	-1.432
4	0.365	-1.357
5	0.352	-1.457
6	0.315	-1.416

As it can be seen from the results, in models 1 to 6, the amplitude attenuation increases once the high permeability/porosity layers move toward the downstream reservoir. However, this pattern is not observed in phase shift results and samples with the layer of high permeability/porosity at the middle show greater phase shift values. The difference between the responses of samples with same layers but different order of placement along the core results in different calculated values of permeability and porosity. In fact models 1 and 3 or 4 and 6 are the same and only the location of upstream and downstream reservoirs are different in them but still a significant difference in their response values is getting observed and this implies the significance of further study on accuracy and application of pressure oscillation technique for heterogeneous and/or anisotropic cases.

4. Conclusions

Laboratory experiments to measure the permeability and porosity using pore pressure oscillation method use analytical formulations that are derived based on simplification assumptions such as homogeneity and isotropy of core samples. Not only these assumptions are not valid for all cases, but also it is not possible to derive analytical formulations for all heterogeneous and anisotropic cases. Therefore, numerical simulation can be used as a robust tool to study different models and investigate the response of core samples to pressure wave in different scenarios. The pressure oscillation method was successfully simulated using COMSOL CFD and it showed excellent agreement with the analytical results. Overall, in CFD modeling with constant time step, models with longer pressure wave period showed less computational errors compared to those with shorter period or higher frequency. It was observed that by increasing the period of pore pressure wave the amplitude attenuation and phase shift decrease. In addition, the results showed in models with the same porosity and permeability, the larger the size of downstream reservoir, the higher the phase shift and amplitude attenuation would be. In order to have less amplitude attenuation and phase shift in laboratory experiments, it is important not to have wave frequency higher than certain values and keep the size of downstream reservoir as small as possible. Finally, three different scenarios in form of 6 models of heterogeneity were defined and simulated. The significant difference in response of each model at downstream reservoir shows the importance of further study on behavior of pressure oscillation method in measuring the permeability and porosity or heterogeneous and/or anisotropic core samples.

5. References

[1] Wang, Y. and Knabe, R. J., Permeability Characterization on Tight Gas Samples Using Pore Pressure Oscillation Method, *PETROPHYSICS*, **52 (6)**, p. 437-443 (2011).

[2] Mokhtari, M., Alqahtani, M., Tutuncu, A., Yin, X., Stress-Dependent Permeability Anisotropy and Wettability of Shale Resources, *Unconventional Resources Technology Conference*, Denver, Colorado, Aug 12-14 (2013).

[3] Brace, W. F., Walsh, J. B. and Frangos, W. J., Permeability of Granite under High Pressure, *Journal of Geophysics*, **73(6)**, p. 2225-2236 (1968).

[4] Boitnott, G. N., Use of Complex Pore Pressure Transients to Measure Permeability of Rocks. *SPE Annual Technical Conference and Exhibition*, San Antonio, Texas, Oct 5-8, (1997).

[5] Jones, S. C., A rapid accurate unsteady-state Klinken-berg permeameter, *SPE Reservoir Evaluation & Engineering*, **12(5)**, p. 383-397 (1972).

[6] Hsieh, P. A., Tracy, J. V., Neuzil, C. E., Bredehoeft, J. D., and Silliman, S. E., A transient laboratory method for determining the hydraulic properties of 'tight' rocks – I. Theory; II. Application, *International Journal of Rock Mechanics and Mining Science*, **18(3)**, p. 245-258 (1981).
[7] Dicker, A. I. and Smits, R. M., A practical approach for determining permeability from laboratory pressure-pulse decay measurements, *International Meeting on Petroleum Engineering*, Tianjin, China, Nov. 21-23 (1988).
[8] Egermann, P., Lenormand, R., Longeron, D., and Zarcone, C., A fast and direct method of permeability measurement on drill cuttings, *SPE Reservoir Evaluation & Engineering*, **8(4)**, (2002)
[9] Kranz, R. L., Saltzman, J. S., and Blacic, J. D., Hydraulic diffusivity measurements on laboratory samples using an oscillating pore pressure method, *International Journal of Rock Mechanics and Mining Science*, **27(5)**, p. 345-352, (1990).
[10] Fischer, G. J., Chapter 8 The Determination of Permeability and Storage Capacity: Pore Pressure Oscillation Method, *International Geophysics*, **51**, p. 187-211 (1992).
[11] Bernabe, Y., Mok, U., and Evans, B., A note on the oscillation flow method for measuring rock permeability, *International Journal of Rock Mechanics & Mining Science*, **43**, p. 311-316 (2006).
[12] Song, I., Rathbun, I., and Saffer, D., Uncertainty analysis for the determination of permeability and specific storage from the pulse-transient technique, *International Journal of Rock Mechanics & Mining Sciences*, **64**, p. 105-111 (2013).
[13] Bennion, D. W., Goss, M. J., A sinusoidal pressure response method for determining the properties of a porous medium and its in-situ fluid, *Fall Meeting of the Society of Petroleum Engineers of AIME*, New Orleans, Louisiana, Oct 3-6 (1971).
[14] Mokhtari M., Tutuncu A.N., and Boitnott G.N., Intrinsic Anisotropy in Fracture Permeability, *Interpretation*, **3(3)**, p. 43-53 (2015).
[15] Mokhtari M. & Tutuncu A.N., Characterization of Anisotropy in the Permeability of Organic Rich Shales, *Journal of Petroleum Science and Engineering*, **133**, p. 496-506 (2015).
[16] Salehi, S., Madani, S.A., Kiran, R., Characterization of drilling fluids filtration through integrated laboratory experiments and CFD modeling, *Journal of Natural Gas Science and Engineering*, **29**, p. 462-468 (2016).
[17] Jin G. et al. Permeability Measurements of Organic-Rich Shale – Comparison of Various Unsteady-State Methods, *SPE Annual Technical Conference and Exhibition*, Houston, Texas, Sep 28-30 (2015).